Nature of Prominences and their role in Space Weather
Proceedings IAU Symposium No. 300, 2013
B. Schmieder, J.-M. Malherbe & S. T. Wu, eds.

doi:10.1017/S1743921313011605

HMI observations of two types of ephemeral regions

Shuhong Yang[1], Jun Zhang[1] and Yang Liu[2]

[1]Key Laboratory of Solar Activity, National Astronomical Observatories, Chinese Academy of Sciences, Beijing 100012, China
email: shuhongyang@nao.cas.cn

[2]W.W. Hansen Experimental Physics Laboratory, Stanford University, Stanford, CA 94305-4085, USA

Abstract. Using the magnetograms observed with the Helioseismic and Magnetic Imager, we statistically study the ephemeral regions (ERs) of the Sun. we notice that the areas with locations around S15° and N25° have larger ER number density, implying that the generation of ERs may be affected by the large-scale background fields from dispersed active regions. According to their evolution, the ERs can be classified into two types, i.e., normal ERs (2798 ones) and self-canceled ERs (190 ones). Submergence of initial magnetic flux loops connecting the opposite dipolar polarities may lead to the self-cancellation.

Keywords. Sun: evolution, Sun: photosphere, Sun: surface magnetism

1. Introduction

The dipolar magnetic field regions in the solar photosphere ranges from smaller than 10^{18} Mx to larger than 10^{23} Mx, and the small short lived ones are named ephemeral regions (ERs; Harvey & Martin 1973). With the magnetograms from the Solar and Heliospheric Observatory (SOHO), Schrijver *et al.* (1998) noticed that the mean total unsigned flux per ER is 1.3×10^{19} Mx. In the quiet Sun, ERs continuously emerge and replenish the magnetic flux loss due to the dispersion and cancellation (Schrijver *et al.* 1998; Hagenaar *et al.* 2003). The Helioseismic and Magnetic Imager (HMI; Scherrer *et al.* 2012) onboard the Solar Dynamics Observatory (SDO; Pesnell *et al.* 2012) uninterruptedly measures the full-disk magnetic fields with a 45 s cadence and a pixel size of 0.5 arcsec. These advantages are very helpful for us to statistically investigate the ERs in the quiet Sun.

2. Observations and Results

In this study, we adopt the HMI line-of-sight magnetograms observed in a four-day period, i.e., from 2010 June 11 12:00 UT to June 15 12:00 UT. We only consider the pixels with heliocentric angle (α) smaller than 60° (delineated by the red circle in Figure 1 (a)). All the magnetograms are differentially rotated to a reference time (2010 June 13 12:00 UT). The blue curve outlined the target with $\alpha < 60°$ during the four days. The area S and the magnetic flux density B of each pixel in the derotated magnetograms are calculated as $S/\cos(\alpha_0)$ and $B/\cos(\alpha_1)$, respectively. Note that α_0 is the heliocentric angle of the pixel, while α_1 is the heliocentric angle at the observation time.

We identify 2988 ERs and their spatial distribution are presented in Figure 1 (a) (marked with blue dots). The target area after projection correction is 8.0×10^5 Mm^2, and thus the mean number density is 9.32×10^{-4} day^{-1} Mm^{-2}. We display the latitudinal

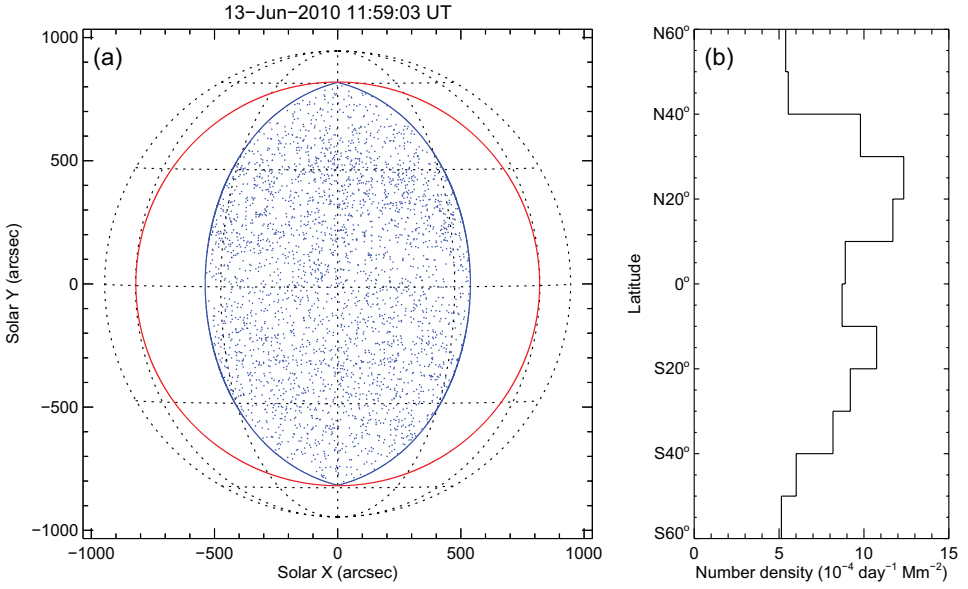

Figure 1. Spatial distribution (left panel) and latitudinal distribution (right panel) of the ERs. The red circle marks the place with heliocentric angle α of 60°, and the blue curve outlines the area with $\alpha < 60°$ during the whole four days.

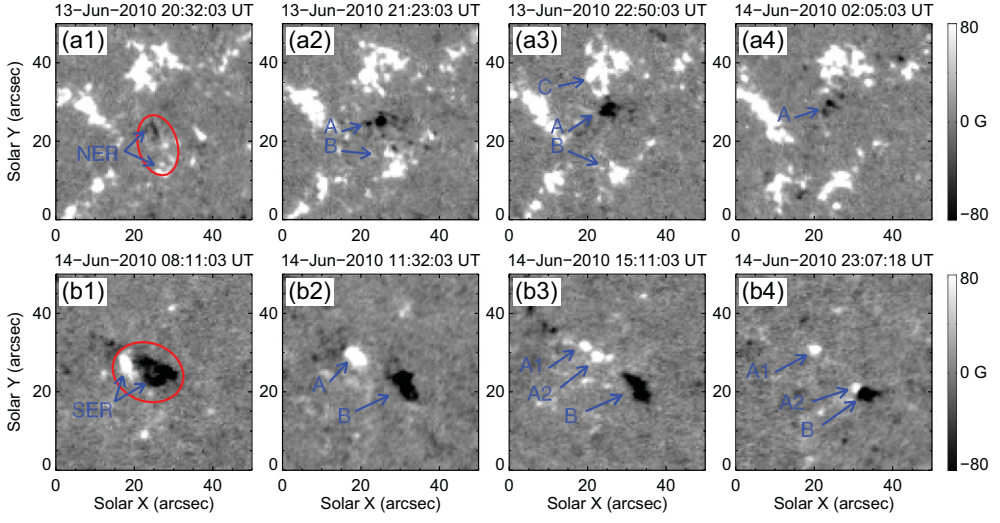

Figure 2. Sequence of magnetograms showing the evolution of an NER (upper panels) and an SER (lower panels). The ellipses outline the areas where the ERs emerged.

distribution of these ERs in Figure 1 (b), and find that the ERs are not distributed uniformly. Two regions have larger number density: one region is around S15° and the other one is around N25°, where the number density exceeds 10×10^{-4} day^{-1} Mm^{-2}. We measure the unsigned magnetic flux of the ERs and find that their mean magnetic flux is 9.27×10^{18} Mx.

According to their performance, these ERs can be classified into two types, i.e., normal ERs (NERs) and self-canceled ERs (SERs), and their numbers are 2798 and 190, respectively. We find that 9.8% of the total flux of ERs disappeared due to the self-cancellation.

https://doi.org/10.1017/S1743921313011605 Published online by Cambridge University Press

The upper panels in Figure 2 show the evolution of an NER. The NER emerged as a dipolar region (marked by arrows in panel (a1)). Then the opposite polarities (denoted by "A" and "B" in panel (a2)) separated, and the negative polarity encountered and canceled with the pre-existing positive field (denoted by arrow "C" in panel (a3)). At 02:05 UT on June 14, most magnetic flux of patch "A" disappeared (panel (a4)). The lower panels display an example of SERs. The ellipse outlines the location of the SER (see panel (b1)). The two patches of the SER (denoted by arrows "A" and "B" in panel (b2)) separated, and the positive patch "A" split gradually into elements "A1" and "A2" (panel (b3)). Patch "A2" moved toward to patch "B" and canceled with it (see panel (b4)).

3. Discussion

As shown in this study, the average unsigned magnetic flux of ERs is 9.3×10^{18} Mx, smaller than that (1.3×10^{19} Mx) determined with the SOHO magnetograms (Schrijver *et al.* 1998). Figure 1 (b) shows that, instead of the high latitudinal and the equatorial regions, the areas located at around S15° and N25° (the general latitudes of active regions) have larger ER number density, implying that the generation of ERs may be affected by the large-scale background magnetic fields from decayed and dispersed active regions.

Zwaan (1978, 1987) illustrated that the retraction of initial magnetic flux loops connecting the two poles into the sub-photosphere can lead to magnetic flux cancellation, an observational phenomenon. Besides the theory, the submergence of a sunspot group was also observed by Zirin (1985). We suggest that the self-cancellation of SERs results from the submergence after emergence of magnetic flux loops connecting the opposite dipolar polarities. When dipolar patches with opposite polarities cancel with the surrounding magnetic fields, magnetic reconnection takes place accompanied with energy release, the flux connection is changed and the magnetic configuration is restructured. While when the initial flux loops submerge after emergence, no magnetic flux reconnection occurs and thus no magnetic energy is released during this process.

Acknowledgements

This work is supported by the Outstanding Young Scientist Project 11025315, the National Basic Research Program of China under grant 2011CB811403, the National Natural Science Foundations of China (11203037, 11221063, 11373004, and 11303049), and the CAS Project KJCX2-EW-T07.

References

Hagenaar, H. J., Schrijver, C. J., & Title, A. M. 2003, *ApJ*, 584, 1107
Harvey, K. L. & Martin, S. F. 1973, *Solar Phys.*, 32, 389
Pesnell, W. D., Thompson, B. J., & Chamberlin, P. C. 2012, *Solar Phys.*, 275, 3
Scherrer, P. H., Schou, J., Bush, R. I., *et al.* 2012, *Solar Phys.*, 275, 207
Schrijver, C. J., Title, A. M., Harvey, K. L., *et al.* 1998, *Nature*, 394, 152
Zirin, H. 1985, *ApJ*, 291, 858
Zwaan, C. 1978, *Solar Phys.*, 60, 213
Zwaan, C. 1987, *ARAA*, 25, 83